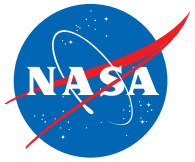

Jet Propulsion Laboratory
California Institute of Technology

ELECTRICAL ENGINEERING
AND COMPUTER SCIENCE
UNIVERSITY OF MICHIGAN

Application of Multi-frequency Tomography Radar Observations for Snow Stratigraphy

Xiaolan Xu[1], Jan-Willem De Bleser[1], Simon Yueh[1],
Haoran Shen[2], Jiyue Zhu[2], Haokui Xu[2], Leung Tsang[2]

[1]Jet Propulsion Laboratory, California Institute of Technology, Pasadena, CA
[2]University of Michigan, Annbor, MI, USA

PIERS
Photonics & Electromagnetics Research Symposium

IGARSS 2019 • Yokohama, Japan, Jul.28 – Aug 2, 2019

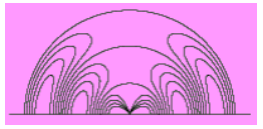

Background

Importance for seasonal snow research

- Over 30% of Earth's total land surface has seasonal snow. Over 60% of the northern hemisphere land surface has snow cover in the mid winter.
- Snow cover (extent, duration, water equivalent) is an indicator for the climate change
- Snowmelt dominate the runoff, affecting about ¼ of the global domestic product.
- Snow is a significant storage component of the global water cycle
- Responsible for flooding

Motivations for snow remote sensing

- Direct ground measurement networks are sparse and limited.
- Remote sensing systems offer a global scale, year-around recorded data
- Fundamental questions need to be understood

Overview

- Introduction
- Tomography Radar System
- Overview of the field experiments
  - Deployment at CUES (CRREL-UCSB Energy) sites, CA
  - Deployment at Fraser Forest sites, CO
- Preliminary results and modeling
- Summary

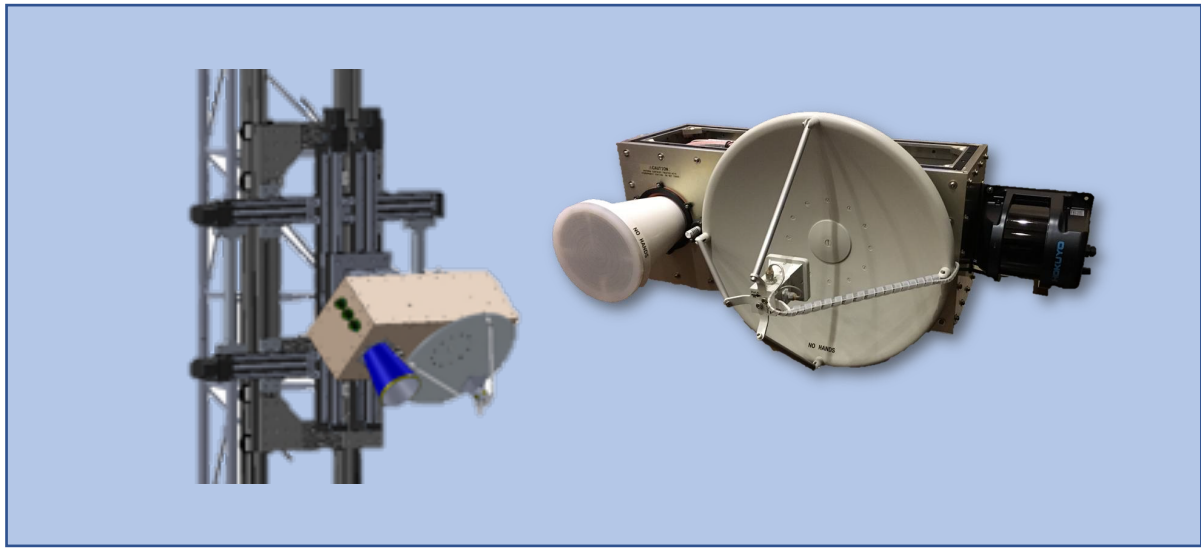

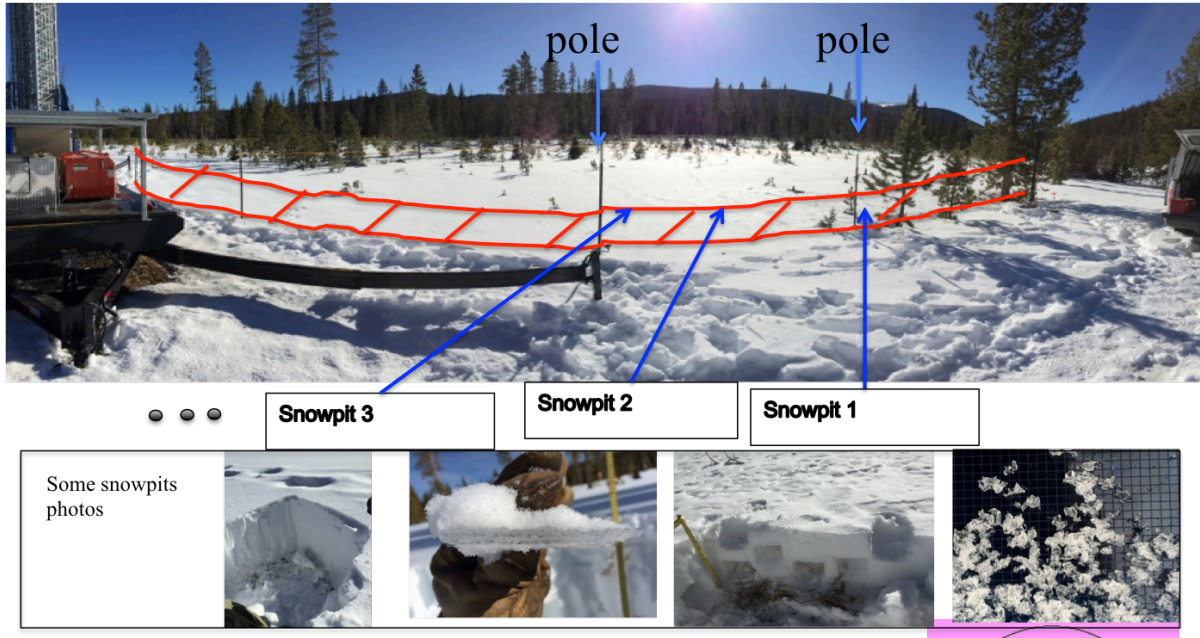

Introduction

- Snow Stratigraphy
  - Traditional measurement: Snow pit
  - Snow reflectance mapping (NIR photography)
- Tomography provides unique access to the structure of the snow
  - Enables the separation of multiple snow layers
  - Detection of and compensation for soil and vegetation layers.
- Polarimetric capabilities
  - Detect spatially varying shapes, sizes, and permittivities
  - Decompose the backscattered signal into volumetric and surface scattering components

Tomography Radar System

1. Three frequencies FMCW radar centered at 9.6 GHz, 13.5 GHz, and 17.2 GHz

2. The transceiver is mounted to a dual-axis planar scanner (60cm in each direction), which creating a tomographic baseline in two directions.

3. Dual-antenna architecture was implemented to improve the isolation between the transmitter and receiver.

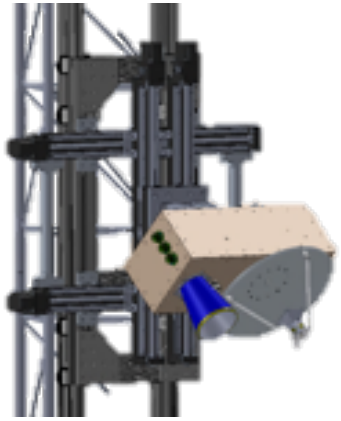

	X	Ku Low	Ku High
Tx Frequency [GHz]	9.35–9.85	13.25–13.75	16.95–17.45
Tx Bandwidth [GHz]	0.5	0.5	0.5
Tx Power [dBm]	0	0	0
Range Resolution [m]	0.3	0.3	0.3
X-pol Isolation [dB]	>30	>30	>30
RCS Sensitivity [dBm^2/m^2]	-55	-55	-55
Horn Beamwidth [deg]	60.3	42.2	35.6
Dish Beamwidth [deg]	5.8	4.1	3.2
Scanning Range [m]	0.6	0.6	0.6

TABLE I

Vertical Resolution

1 look ..... 12 look

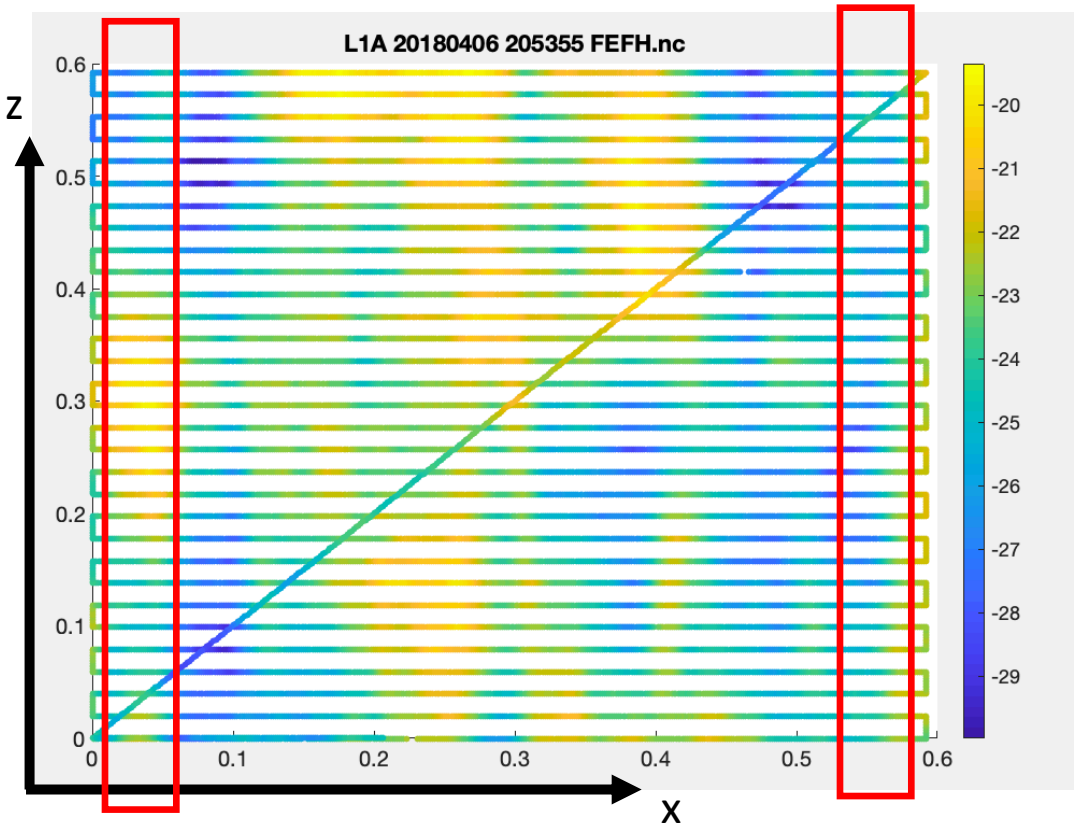

Cross Range Aperture
L = 0.6/√2m

$$\delta_n = \frac{\lambda}{2L} R$$

$$\delta_r = \frac{c}{2B} = 30cm$$

Deployment at CUES site, CA

- The system was deployed on a snow study site mid way up Mammoth Mountain managed by UCSB (37.643°N, 119.029°W)
- In situ measurements of snow depth and other snowpack properties were recorded automatically every day. LiDAR scans the snow surface every 15min
- Time
  - Apr. 17- Jun 20, 2016

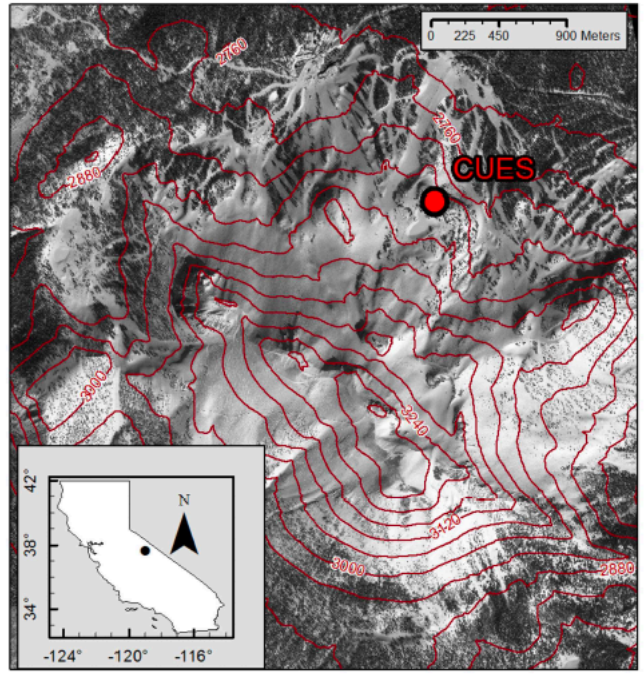

Deployment at Fraser, CO

- The system was deployed on a ground based tower at the Fraser Experimental Forest (FEF) Headquarters, near Fraser, CO, USA (39.847°N, 105.912°W)
- In situ measurements of snow depth and other snowpack properties were performed every week for comparison with the remotely sensed data
- Time
  - Feb.1 – May 30, 2017
  - Jan.15 – May 1, 2018

Field setup

CUES Mammoth Lakes, CA

Fraser, CO

f(GHz)	δ_r(m)	λ(m)	L (m)	δ_n(m)	δ_z		L (m)	δ_n(m)	δ_z(m)
9.6	0.3	0.031	0.6	0.234	0.378		0.424	0.365	0.470
13.5	0.3	0.022	0.6	0.167	0.330		0.424	0.259	0.395
17.2	0.3	0.017	0.6	0.131	0.305		0.424	0.203	0.356

Data processing

- Multi-looking time-domain back-projection processor

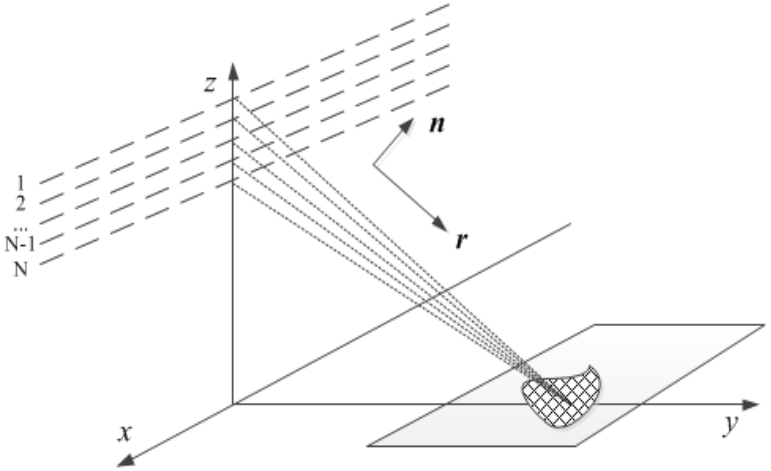

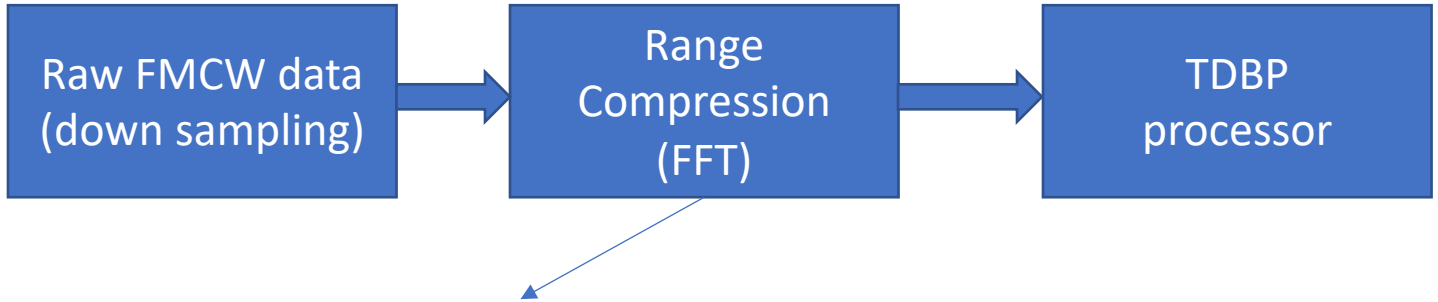

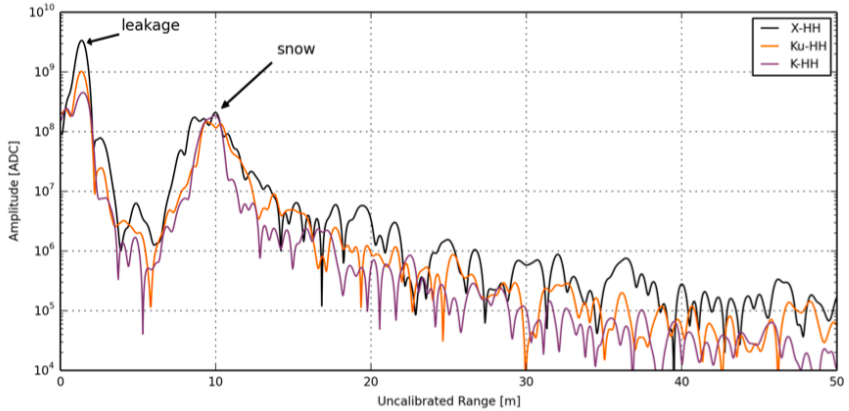

$$I(\bar{p}) = \sum_{n=1}^{N} S_n(\bar{p}) e^{-i\phi_n(\bar{p})}$$

N is the total number of transmitter-receiver pairs

$\bar{p}$ represents a certain point in the ground range and height plane

$S_n(\bar{p})$ is range compressed signal sampled focused at position $\bar{p}$

$\phi_n(\bar{p})$ is the phase compensation term for the target position $\bar{p}$

$$\phi_n(\bar{p}) = k_c(|r_n^{Tx} - \bar{p}| + |r_n^{Rx} - \bar{p}|)$$

where k_c is the wavenumber at center frequency.

CUES site: Time-series analysis

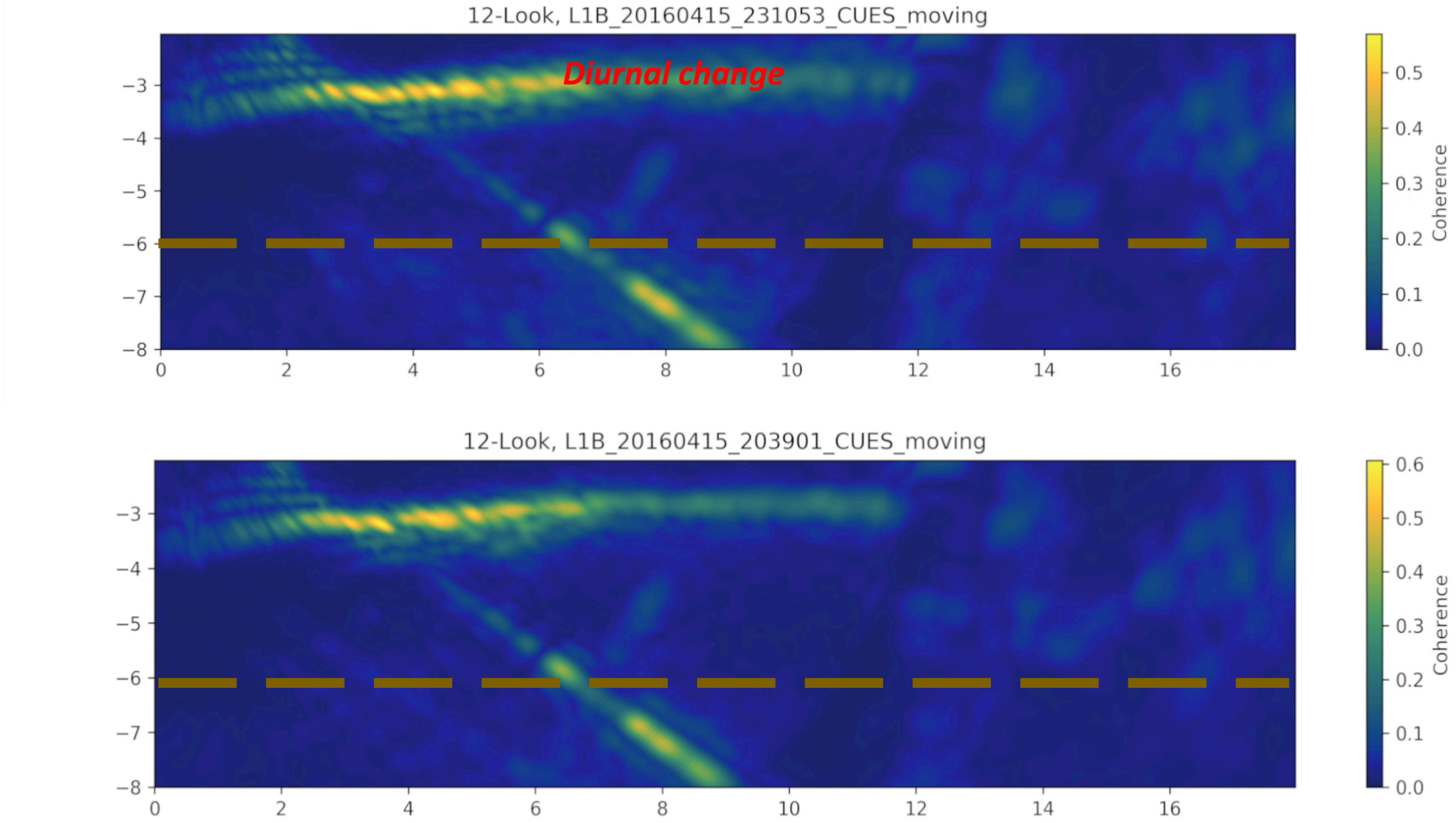

Three-frequency & full-polarized capabilities

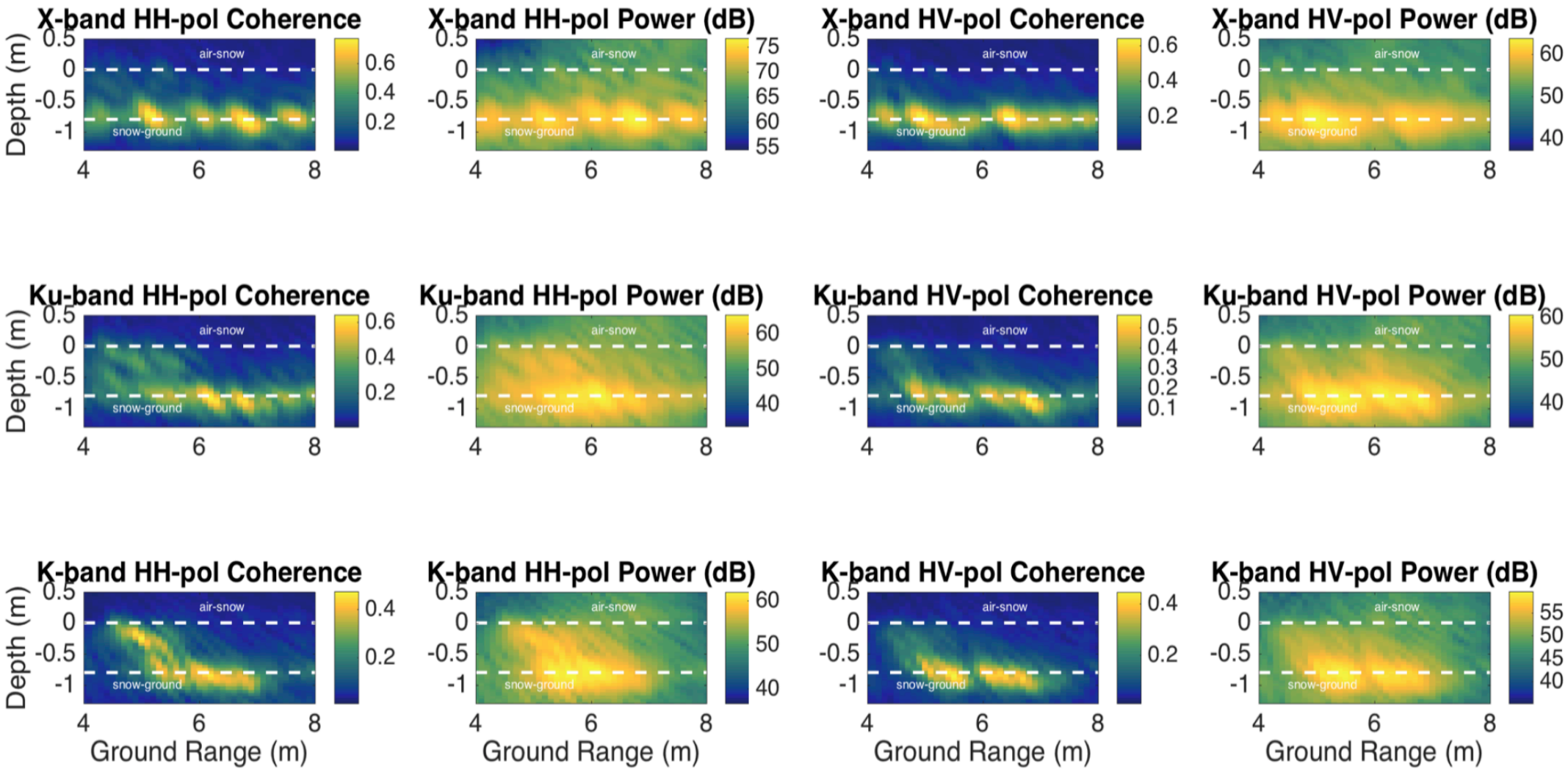

Snow Stratigraphy from Tomograms

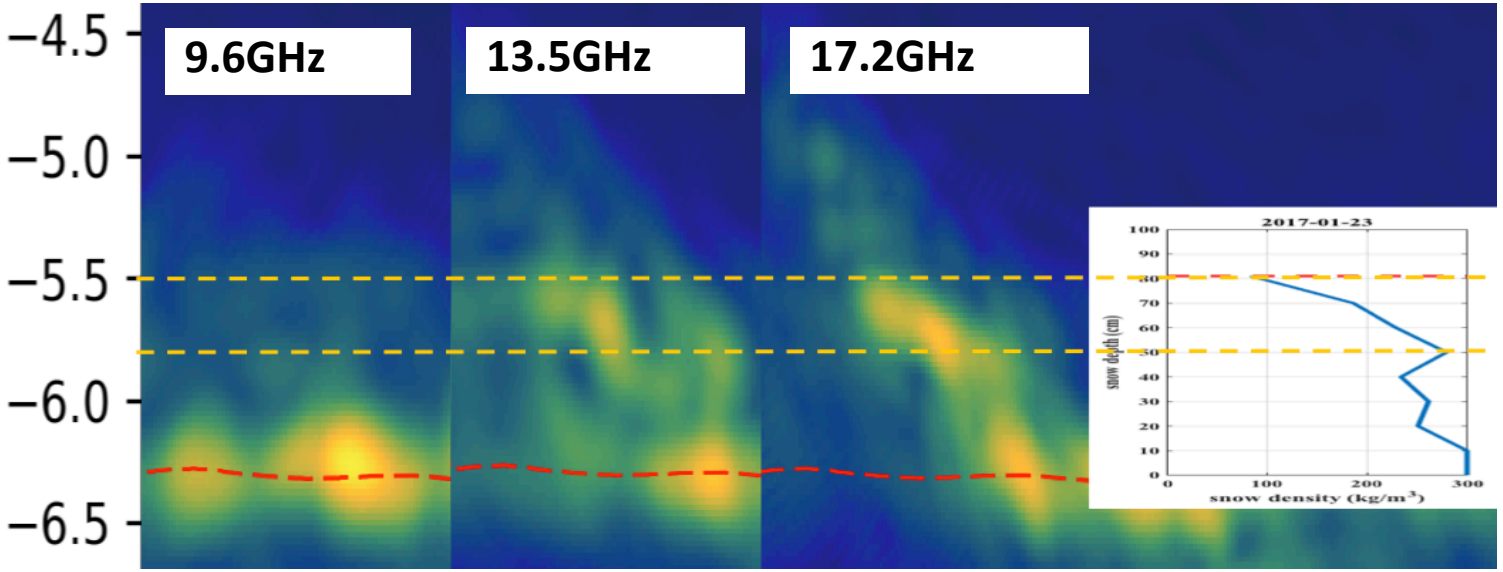

1. The red line is ground reference position derived from the snow-free laser measurement. The plot demonstrates the coherency of the vertical slice.

2. As the frequencies increases, the volume scattering from the snow become more prominent.

3.The snow density of the pit measurement also matches coherency distribution.

Coherence profiles extracted from the averaged main-lobe tomograms

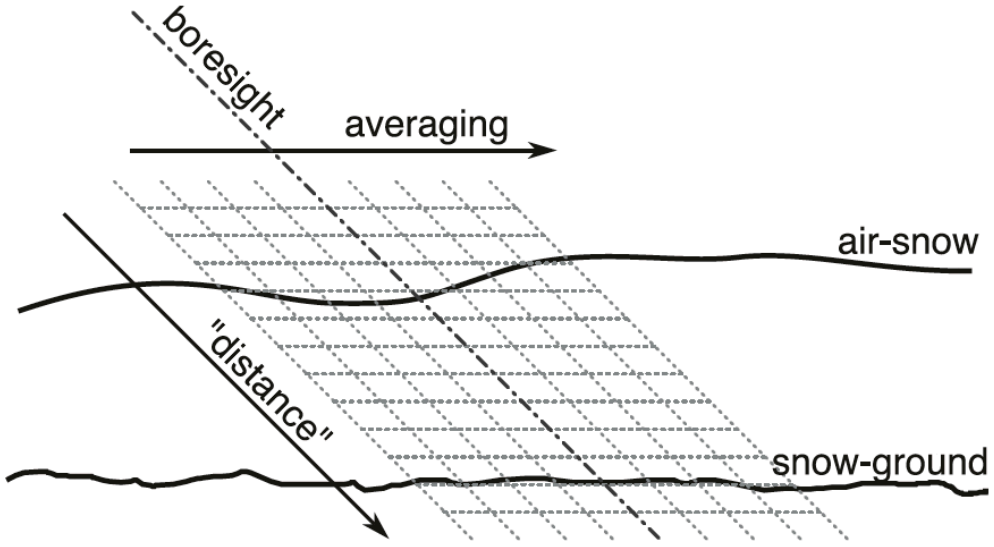

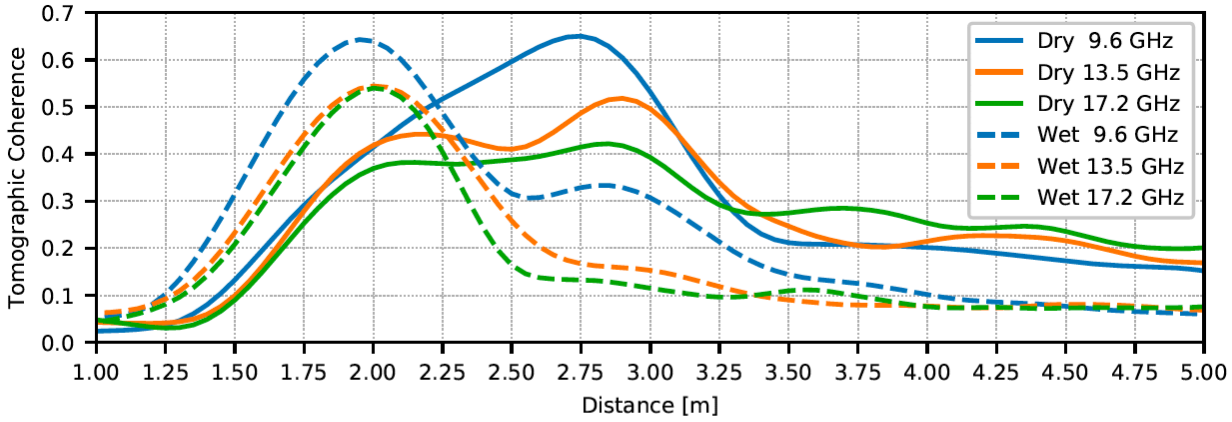

(a) HH

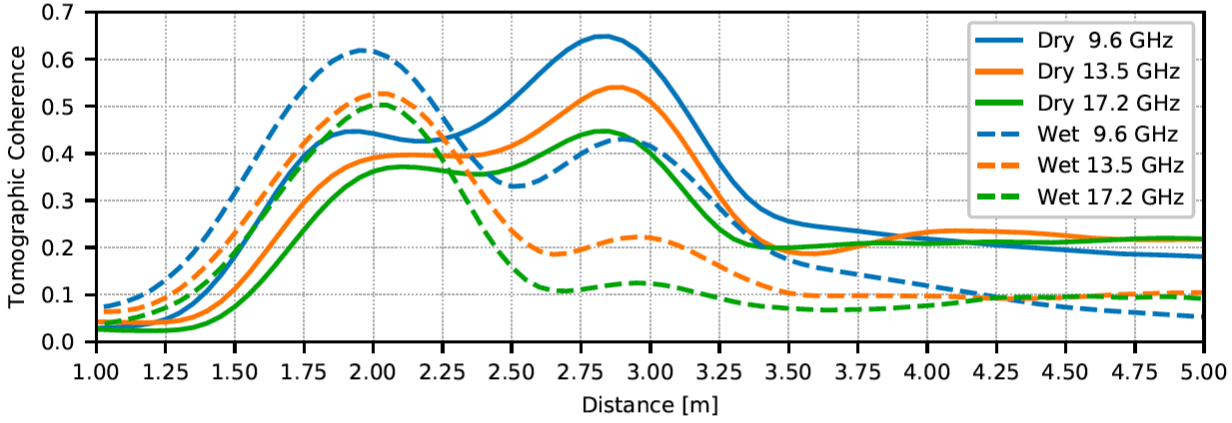

(b) VV

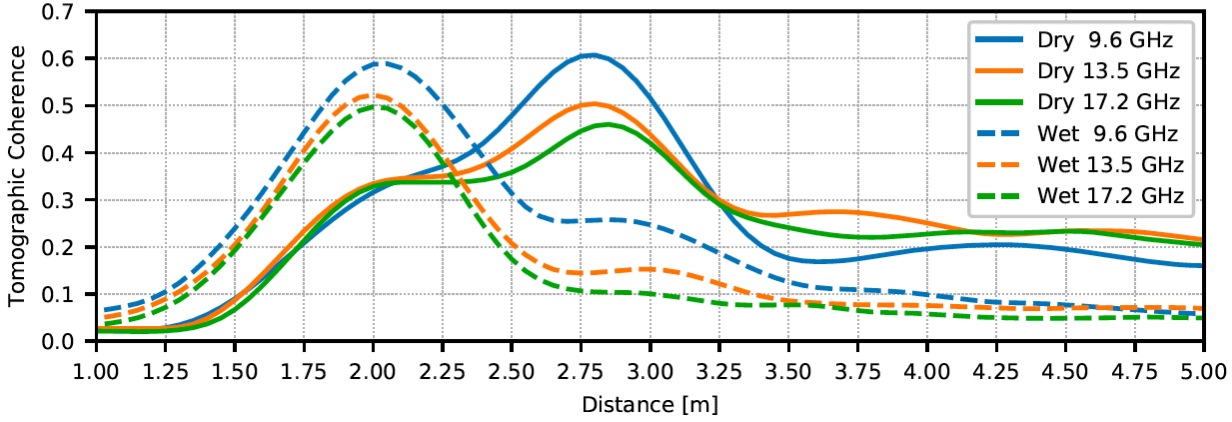

3D tomograms

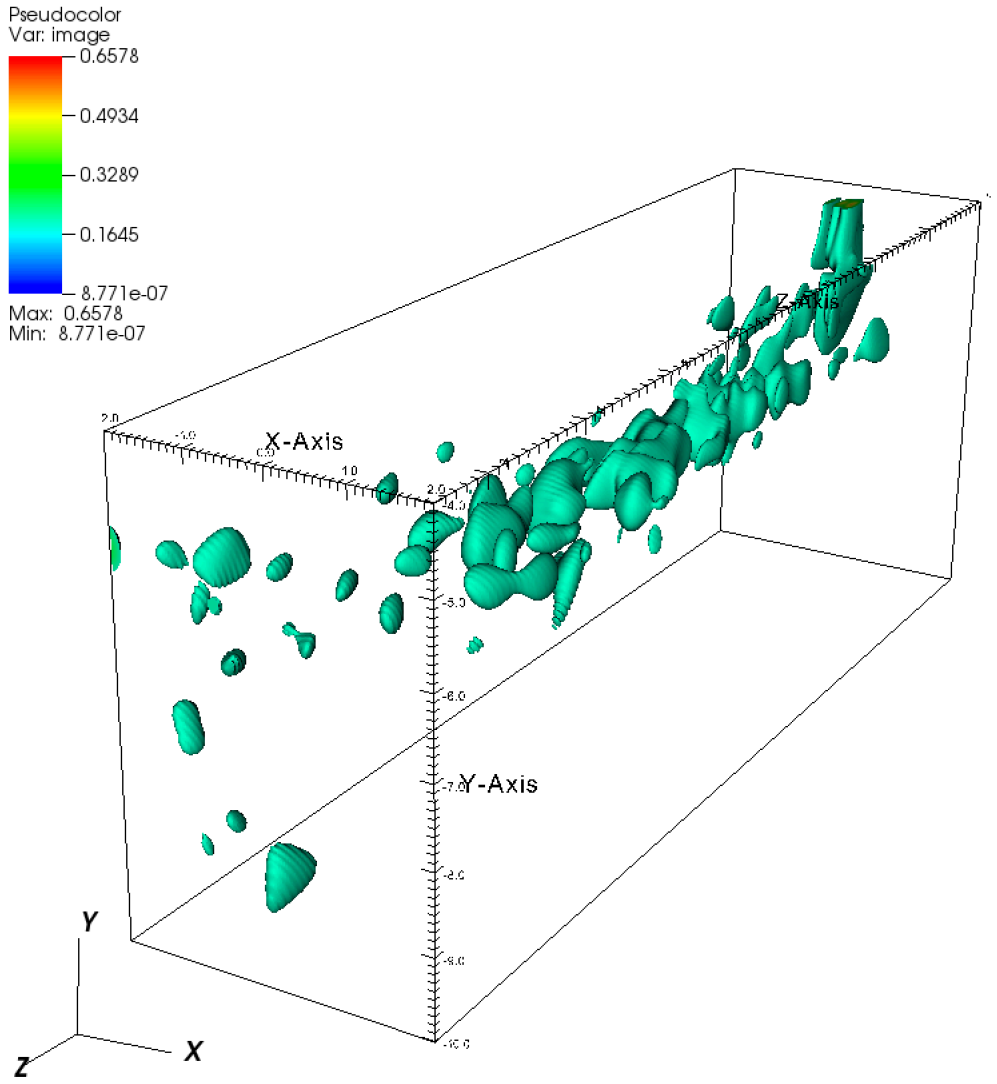

Analytical modeling using Born approximation

- Incident field: $\psi_{inc} = \psi_0 \exp(ik \sin\theta_0 x - ik \cos\theta_0 z)$

- Born's approximation for small object:

$$\psi_s = k^2 \frac{i}{4} H_0^{(1)}(k|\vec{\rho} - \vec{\rho}'|) p' \qquad p' = \Delta s(\varepsilon_r(\vec{\rho}) - 1)\psi_{inc}$$

- In the far field:

$$\psi_s = k^2 \sqrt{\frac{1}{\rho}} \exp(ik\rho) \exp(-i\vec{k_s}.\vec{\rho}') \sqrt{\frac{2}{\pi k}} \exp(i\frac{\pi}{4})[\psi_0 \exp(i\vec{k_i}.\vec{\rho}')\Delta s(\varepsilon_r(\vec{\rho}') - 1)]$$

$$\vec{\rho} = (x, z) \qquad \vec{k_i} = (k\sin\theta, -k\cos\theta) \qquad \vec{k_s} = (-k\sin\theta, k\cos\theta)$$

- For position $\vec{\rho}'$ define a scattering amplitude:

$$f_{sd}(\vec{\rho}') = k^2 \frac{i}{4} \sqrt{\frac{2}{\pi k}} e^{-i\frac{\pi}{4}} \left(\varepsilon_r(\vec{\rho}') - 1\right) \Delta s$$

Imaging Equations (1)

- For many small objects without multiple scattering:

$$\psi_s = \sqrt{\frac{1}{\rho}} \exp(ik\rho)\psi_0 \sum_j f_{sd}(\vec{\rho}_j) \exp(i2k \sin\theta x_j - i2k \cos\theta z_j)$$

- Scattering amplitude for all the objects:

$$f(k,\theta) = \sum_j f_{sd}(\vec{\rho}_j) \exp(i2k \sin\theta x_j - i2k \cos\theta z_j)$$

- To find the $f_{sd}(\vec{\rho}_j)$:

$$f_{sd}(\vec{\rho}_j) = \frac{1}{N_k}\frac{1}{N_\theta}\sum_m \sum_n f(k_m,\theta_n) \exp(-i2k_m \sin\theta_n x_j + i2k_m \cos\theta_n z_j)$$

Imaging Equations (2)

- Previously we looked for $$O(\vec{\rho}_j) = \Delta s \frac{i}{4}\sqrt{\frac{2}{\pi}}\exp(-i\frac{\pi}{4})(\varepsilon_r(\vec{\rho}_j)-1)$$

$$O(\vec{\rho}_j) = \frac{1}{N_k}\frac{1}{N_\theta}\sum_m\sum_n \frac{1}{k_m^{1.5}} f(k_m,\theta_n)\exp(-i2k_m \sin\theta_n x_j + i2k_m \cos\theta_n z_j)$$

- In comparison with $f_{sd}(\vec{\rho}_j)$

$$f_{sd}(\vec{\rho}_j) = \frac{1}{N_k}\frac{1}{N_\theta}\sum_m\sum_n f(k_m,\theta_n)\exp(-i2k_m \sin\theta_n x_j + i2k_m \cos\theta_n z_j)$$

- f is obtained from DDA for imaging
  - multiple scattering effect is included
  - Imaging process treat it as single scattering

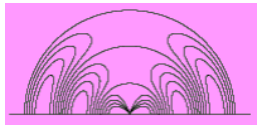

2D SAR tomography using Bicontinuous model (numerical simulation)

- Top layer:
  - zeta:10000
  - b:2
  - Volume fraction:0.15
  - Grain Size: 1mm
- Bottom layer
  - zeta:5000
  - b:1
  - Volume fraction:0.3
  - Grain Size: 2mm

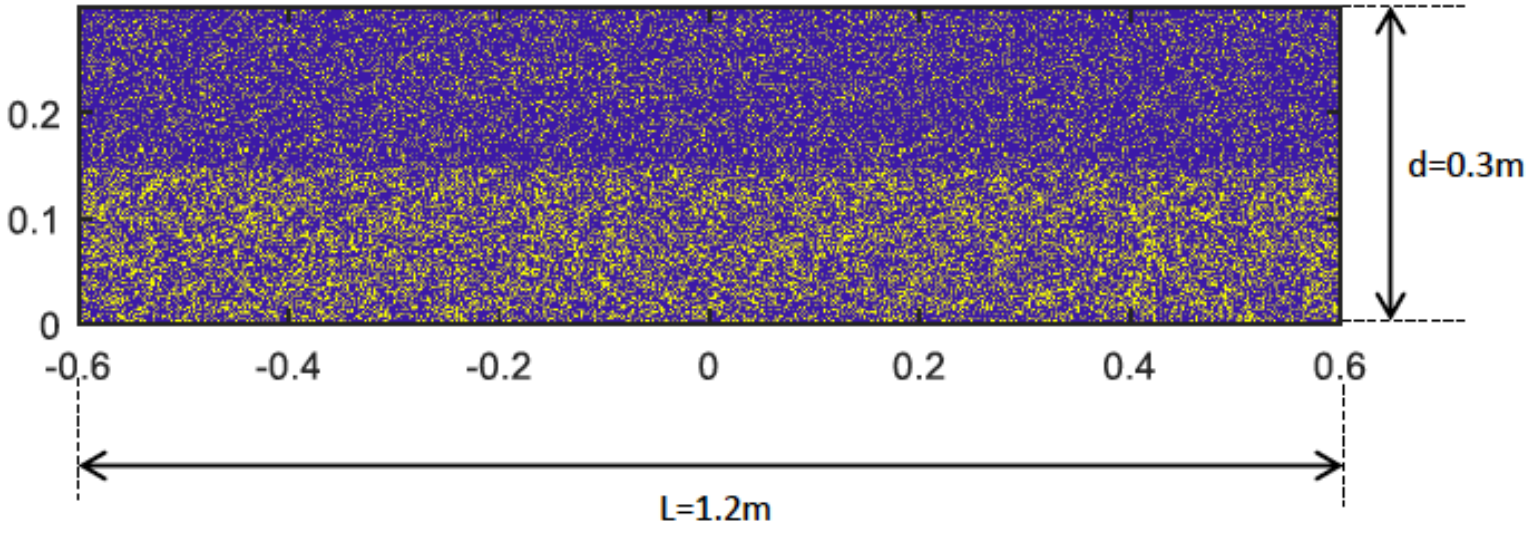

Modeled tomography (O) of the snowpack:

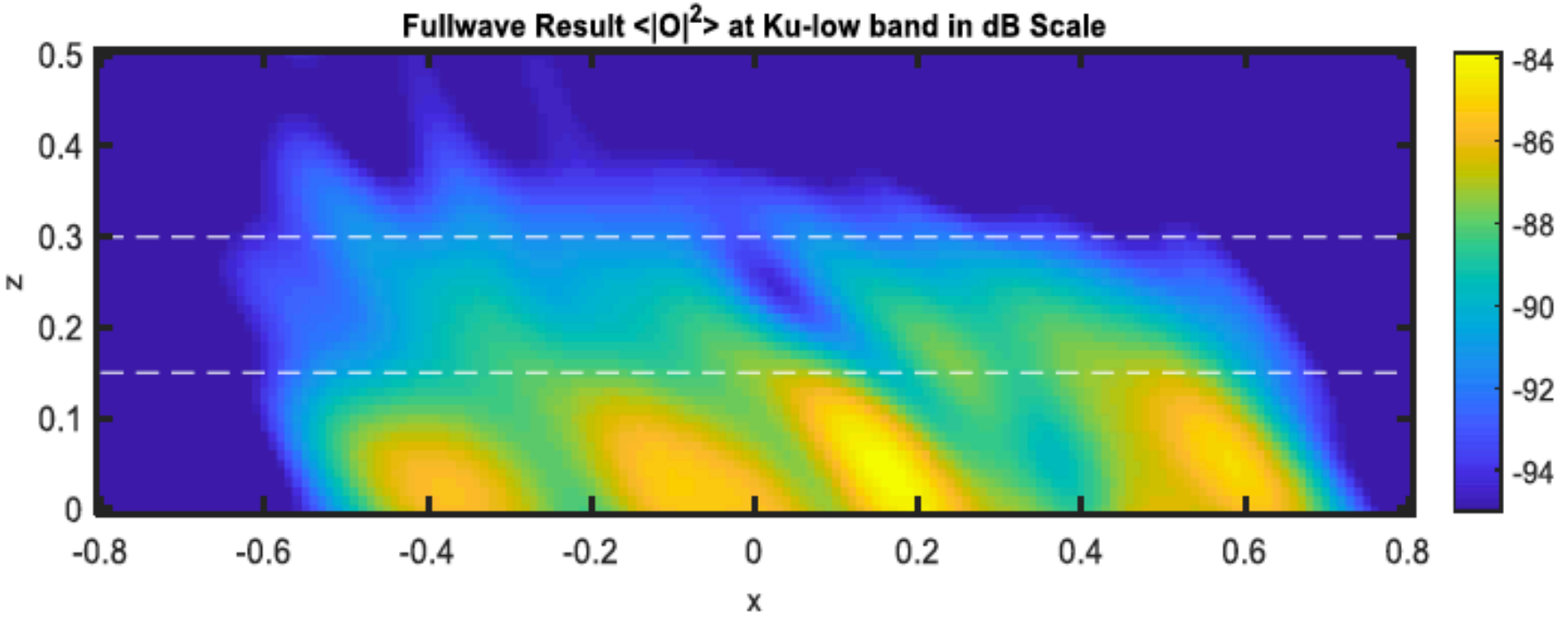

Parameters	Value
Thickness (d)	d = 0.3m, d1=d2=0.15m
Length (L)	L = 1.2m
Wavelength	λ = 0.022m (Ku-low)
Permittivity	$\varepsilon_r = 3.2$

Summary

- Overview of Radar setup
- Clearly diurnal change
- Preliminary Results for 2D modeling

Future work

- Test various radar techniques for SWE retrieval: SAR tomography, InSAR/PolInSAR, etc
- Cross-validate other field & remote sensing data at the Fraser site